

Measuring dopant concentrations in p-type silicon using iron-acceptor pairing monitored by band-to-band photoluminescence

S.Y. Lim*, D. Macdonald

School of Engineering, College of Engineering and Computer Science, The Australian National University, Canberra ACT 0200, Australia

ARTICLE INFO

Article history:

Received 26 October 2010

Received in revised form

18 March 2011

Accepted 21 April 2011

Available online 20 May 2011

Keywords:

Silicon solar cells

Band-to-band photoluminescence

Iron-acceptor pairs

Dopant concentration

ABSTRACT

This paper introduces a photoluminescence-based technique for determining the acceptor concentration in silicon wafers by measuring the formation rate of iron-acceptor pairs. This rate is monitored by band-to-band photoluminescence in low injection, the intensity of which is proportional to the carrier lifetime. The technique is demonstrated with an iron-implanted float zone silicon wafer, heavily compensated Czochralski-grown silicon wafers with iron contamination and an upgraded metallurgical-grade silicon wafer containing natural iron. The FeB pairing rates measured on the float zone sample at different temperatures yield an activation energy that correlates closely to the migration enthalpy associated with the diffusion of iron in silicon, confirming that the changes observed are indeed due to iron-acceptor pairing. The acceptor concentrations determined in the strongly compensated Czochralski-grown silicon wafers and the upgraded metallurgical silicon wafer using the new technique were consistent with the values obtained by the Quasi-Steady-State Photo Conductance lifetime measurement technique and inductively coupled plasma mass spectroscopy respectively, thus proving its usefulness.

© 2011 Elsevier B.V. All rights reserved.

1. Introduction

It is well known that iron, one of the most common impurities in silicon solar cell materials, has a detrimental impact on the minority carrier lifetime due to the defect states introduced by iron and its complexes with acceptors in the band gap of silicon [1]. This paper exploits the reaction kinetics of iron with shallow acceptors, to obtain information on the dopant concentration of the silicon substrate via band-to-band photoluminescence. This non-destructive way of obtaining dopant concentrations can be used in the analysis of low cost silicon materials, irrespective of the presence of dopant compensation [2].

It is known that Fe_i and FeB impurities exist in equilibrium proportions in silicon at a given temperature [3]. When the equilibrium state is perturbed by external stimulation, for example by optical or thermal activation, the resulting Fe_i concentration will resume its equilibrium proportions through an exponential decay with a time constant that is determined by the diffusivity of interstitial Fe, the dopant concentration and the temperature [4,5]. This results in a direct correlation between the FeB re-pairing time constant and the dopant concentration at any given temperature.

As the pairing of Fe_i with acceptor atoms has a clear signature on the carrier lifetime of p-type silicon, time-resolved lifetime measurements using conventional lifetime techniques can be

used to determine the total acceptor concentration. A technique has been proposed in recent years to conduct such measurements using Quasi-Steady-State Photo Conductance lifetime measurements (QSSPC) [2]. This paper proposes another technique based on the steady-state band-to-band photoluminescence intensity, which has some distinct advantages since it is more easily applicable under true low injection conditions.

Monitoring the band-to-band photoluminescence intensity is a highly sensitive method for measuring the excess carrier lifetime. It can be performed in transient mode [6], quasi-steady-state (QSSPL) [6] or true steady state (SS), as is done with the recent photoluminescence imaging technique [7]. QSS and SS PL lifetime measurements can be performed down to injection levels as low as $1 \times 10^9 \text{ cm}^{-3}$ [8]. Such photoluminescence measurements are unaffected by various experimental artefacts caused by minority carrier trapping and depletion region modulation at low injection, as opposed to QSSPC [9]. This provides a clear advantage in this context, since it allows steady-state PL measurements lasting for many seconds to be performed without breaking FeB pairs during the measurement itself, which would otherwise result in an incorrect determination of the re-pairing time constant [4]. This is due to the fact that the pair breaking rate is proportional to the square of the generation rate [10], and so measurements performed with weak generation rates, which corresponds to low injection, can avoid significant iron-acceptor pair breaking.

Lastly, it is worth noting that monitoring of iron-acceptor kinetics can be carried out over a wide range of temperatures. Experiments carried out at higher temperature will result in a shorter observation time frame needed to capture the full

* Corresponding author.

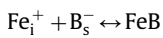
E-mail address: siew.lim@anu.edu.au (S.Y. Lim).

dynamic process of the association; conversely, a lower temperature will result in a longer observation time window. This flexibility becomes useful when measuring samples that contain very high acceptor concentration (e.g. $\gg 1 \times 10^{16} \text{ cm}^{-3}$) or very low acceptor concentration (e.g. $\ll 1 \times 10^{16} \text{ cm}^{-3}$).

2. Theory

2.1. The iron–boron reaction kinetics

The kinetics of the iron–boron pairing is described by [11]



FeB is dissociated when the equilibrium is perturbed by illumination, heating or carrier injection. Once the excitation source is removed, the resulting Fe_i relaxes to the paired equilibrium state with a time constant τ_{assoc} that is dopant density and temperature dependant [4]

$$\tau_{\text{assoc}} = \frac{BT}{N_A} \exp\left(\frac{0.66}{kT}\right) \quad (1)$$

where the constant $B = 5.7 \times 10^5 \text{ s/K cm}^3$ [12]. The temperature T is in Kelvin (several temperatures were used in this study), N_A is the acceptor concentration (cm^{-3}), Boltzmann's constant $k = 8.617 \times 10^{-5} \text{ eV/K}$ and τ_{assoc} is in units of seconds.

If we define the relative instantaneous interstitial iron concentration $\text{Rel}[\text{Fe}_i](t)$ as

$$\text{Rel}[\text{Fe}_i](t) = \frac{[\text{Fe}_i](t)}{[\text{Fe}_i](t) + [\text{FeB}](t)} \quad (2)$$

then the reduction in the relative iron concentration $\text{Rel}[\text{Fe}_i](t)$ can be described by a first order exponential decay equation as follows:

$$\text{Rel}[\text{Fe}_i](t) = \exp\left(-\frac{t}{\tau_{\text{assoc}}}\right) \quad (3)$$

The absolute instantaneous interstitial iron concentration $[\text{Fe}_i](t)$ during pairing is given by [13,14]

$$[\text{Fe}_i](t) = C \left(\frac{1}{\tau(t)} - \frac{1}{\tau_f} \right) \quad (4)$$

where C is a prefactor dependant on the dopant density and excess carrier density, $\tau(t)$ is the instantaneous lifetime and τ_f is the lifetime measured after complete re-pairing of FeB.

The association time constant τ_{assoc} can then be derived from the slope of a plot of $\ln((1/\tau(t)) - (1/\tau_f))$ versus t .

The extraction of the re-pairing rate constant (and thus N_A) using the relative iron concentration, $\text{Rel}[\text{Fe}_i](t)$ means that careful calibration of the PL intensity to determine the absolute values of the generation rate and carrier lifetime is not necessary.

2.2. Photoluminescence technique

The measured photoluminescence intensity, or count rate, I_{PL} (s^{-1}) is proportional to the rate of radiative recombination, R_{rad} and is thus proportional to the product of the minority and majority carrier densities.

$$I_{\text{PL}} = A_i B n p \approx A_i B \Delta n (N_A + \Delta n) \quad (5)$$

where A_i is a scaling factor, B the radiative recombination coefficient and N_A denotes the bulk dopant concentration for non-compensated p-type silicon [8]. At low injection, when $\Delta n \ll N_A$, $I_{\text{PL}} = A_i B \Delta n N_A$. Thus, I_{PL} depends linearly on Δn [8,15].

Since in steady-state, $\Delta n = G\tau$, where G is the generation rate ($\text{cm}^{-3} \text{ s}^{-1}$), then I_{PL} is simply proportional to τ , and we may

extract the association time constant from the exponential decay of I_{PL} itself.

3. Experimental

The primary test sample was a $0.88 \Omega \text{ cm}$, 0.0209 cm thick boron-doped float zone wafer. After initial surface etching and cleaning, the sample was subjected to implantation of 70 keV Fe ions with a dose corresponding to a target volume concentration of $8.2 \times 10^{11} \text{ cm}^{-3}$ in the central area of size $30 \times 30 \text{ mm}^2$. After RCA cleaning, the wafer was then annealed at 1173 K (900 °C) for 60 min in nitrogen to distribute the Fe evenly through the sample. The solubility of Fe in silicon at 1173 K (900 °C) is $4 \times 10^{13} \text{ cm}^{-3}$ [1], so precipitation or out-diffusion of iron could be avoided. SiN films were then deposited by Plasma-Enhanced Chemical-Vapour Deposition (PECVD) on both surfaces, to allow sensitive measurement of the bulk lifetime. The other samples were two strongly compensated Czochralski silicon wafers, which contained iron that was deliberately introduced by annealing at high temperature with some iron contaminated wafers [16] and a p-type CZ wafer made from heavily doped Upgraded Metallurgical-Grade Silicon (UMG-Si), which contained natural concentrations of Fe.

PL measurements were obtained with a BT Imaging LIS-R1 system. During photoluminescence measurement, steady-state carrier generation was achieved with an 808 nm laser diode array with adjustable intensity. The band-to-band photoluminescence radiating from the samples was detected by a one megapixel silicon charge-coupled device camera through a filter that eliminates laser illumination reflected from the sample [17]. The photoluminescence count rate was averaged over several square centimetres of the sample in order to produce an improved signal to noise ratio.

FeB dissociation was achieved by illuminating the samples with multiple flashes of intense white light (≈ 400 suns peak intensity) of 10 ms duration. The PL intensity was recorded as a function of time after the initial lifetime measurement at $t=0$, the time when the last flash was terminated.

The temperature of the sample was monitored using an infrared thermometer to keep track of any possible temperature fluctuations in the sample that were caused by either illumination with the laser diode array, or the surrounding environment. The temperature variation was found to be within $\pm 1 \text{ K}$. A control experiment was also performed on the sample without applying the initial FeB pair breaking illumination to evaluate the noise in the PL count rate at constant temperature. An uncertainty of 1% was obtained. Other sources of uncertainty include the measurement of τ_f and the thermometer sensitivity limit, which constitute a further 2–3% uncertainty. The cumulative effect of these uncertainties propagates through the computation of τ_{assoc} and results in the uncertainty ranges represented in Fig. 4. Lower temperatures were achieved by immersing the samples in chilled or icy water.

4. Results and discussion

4.1. Fe-implanted float zone silicon wafer

4.1.1. Deriving the iron–boron re-pairing time constant

Fig. 1 shows the time-resolved average PL count rate of a $30 \times 30 \text{ mm}^2$ section of the iron-implanted boron-doped FZ sample. The incident photon flux was $1.0 \times 10^{16} \text{ cm}^{-2} \text{ s}^{-1}$. The total acquisition time per data point was 6 s, which is small compared to the time intervals. Assuming an optical absorption factor of 0.6, the average generation rate was found to be

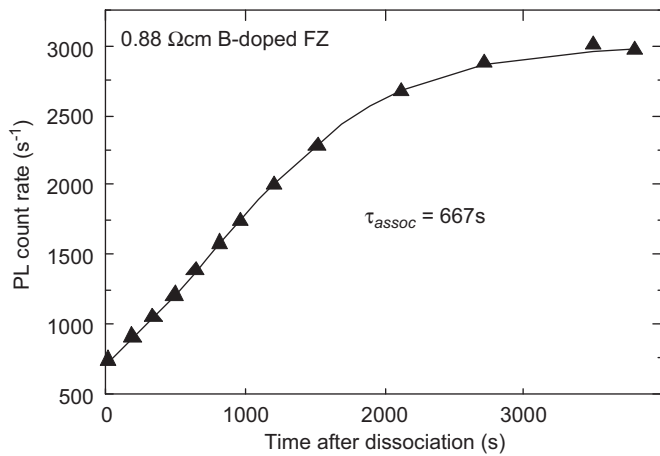


Fig. 1. Time-resolved low injection PL count rate obtained at 307 K (34 °C) from an iron-implanted boron-doped FZ sample. The increase in PL count rate as a function of time reflects the re-pairing of FeB pairs.

around $2.9 \times 10^{17} \text{ cm}^{-3} \text{ s}^{-1}$. Given the upper limit of the sample wafer lifetime, which is 15 μs , this gives a maximum excess carrier concentration Δn value of $4.4 \times 10^{12} \text{ cm}^{-3}$, which is well below the crossover point of the Fe_i and FeB characteristic lifetime signatures [17], and represents low injection conditions. It can be seen that the PL count rate for this sample increased as a function of time during the FeB association process, consistent with being below the crossover point [18]. The solid line is a fit corresponding to a single exponential with a time constant τ_{assoc} of 667 s. The wide range of PL count rate spanned by the measurement, courtesy of the fact that the sample is dominated by the presence of Fe, has rendered the measurement quite insensitive to noise, resulting in a clear exponential fit as shown in Fig. 2.

4.1.2. Comparing with quasi-steady-state (QSSPC) technique

Also shown in Fig. 2. is the decay in $\text{Re}[\text{Fe}_i](t)$ and the corresponding τ_{assoc} value obtained from QSSPC [2] at 307 K (34 °C). The QSSPC lifetimes were extracted at mid-injection ($\tau_{\text{assoc}} = 1 \times 10^{15} \text{ cm}^{-3}$) whereas PL was conducted at low injection. Since the injection level for the QSSPC data was above the FeB crossover point, the QSSPC lifetime decreased with time, as opposed to the PL counts. Nevertheless, the QSSPC data resulted in a similar τ_{assoc} of 703 s. The close correlation between the two results reveals the fact that the PL measurements, which were performed in true low injection conditions, make it possible to obtain a close approximation of τ_{assoc} due to the injection independent characteristics of the carrier lifetime in low injection. From the modelled carrier lifetime versus excess carrier concentration graph in Fig. 3, one can see that changes in excess carrier concentration have little influence on the carrier lifetime in low injection below $1 \times 10^{13} \text{ cm}^{-3}$ as reflected by the flattened curves. Under such conditions, τ_{assoc} extracted at a fixed generation rate (shown by the angled arrow) will reflect the value extracted at a fixed excess carrier density Δn . Hence PL, which operates at low injection can in principle be used to provide a good estimation of τ_{assoc} . This experiment has shown that measurement below an excess carrier concentration of 10^{13} cm^{-3} resulted in a discrepancy of only 6%, which is acceptably small. The energy levels and capture cross sections for Fe_i and FeB are taken from Ref. [16].

Fig. 4 shows an Arrhenius plot of the pair formation rate (proportional to $1/\tau_{\text{assoc}}$) as a function of inverse temperature for the 0.88 $\Omega \text{ cm}$ boron-doped float zone wafer measured at 273 K

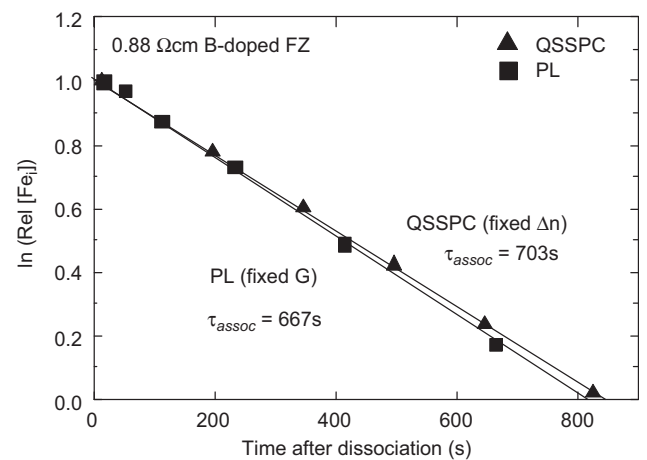


Fig. 2. τ_{assoc} derived from Fig. 1 (PL technique-fixed generation rate) showing good agreement with the τ_{assoc} ($=703 \text{ s}$) obtained using QSSPC (fixed Δn) at 307 K (34 °C).

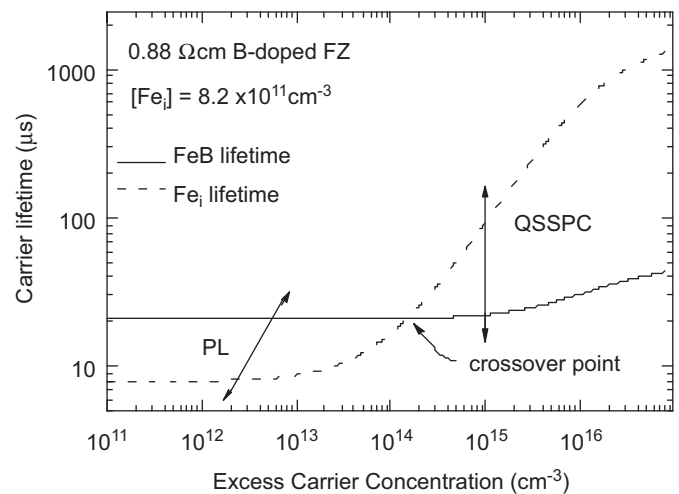


Fig. 3. Modelled carrier lifetimes due to Fe_i and FeB in 0.88 $\Omega \text{ cm}$ boron-doped p-type silicon with an iron concentration of $8.2 \times 10^{11} \text{ cm}^{-3}$ as a function of the excess carrier concentration Δn [17]. The angled arrow next to PL indicates a constant generation rate measurement technique (G). In contrast, the vertical arrow next to QSSPC denotes a fixed Δn technique.

(0 °C), 291 K (18 °C) and 307 K (34 °C). The activation energy derived from the slope was $0.66 \pm 0.03 \text{ eV}$, a value corresponding closely to the known migration enthalpy of interstitial iron in crystalline of silicon [1,19], which is 0.67–0.68 eV. This correlation demonstrates that the reaction we are observing is indeed Fe-acceptor pair formation, and that the formation reaction is limited by the diffusion of Fe, as is known to be the case [4]. The N_A value derived in this experiment via the extracted τ_{assoc} was $1.8 \times 10^{16} \text{ cm}^{-3}$, which is consistent with the N_A result ($1.7 \times 10^{16} \text{ cm}^{-3}$) obtained from the resistivity measured via the dark conductance (0.88 $\Omega \text{ cm}$).

4.2. Compensated Czochralski silicon wafers

The band-to-band photoluminescence technique was applied to two heavily compensated passivated Czochralski-grown silicon (Cz-Si) wafers doped with boron and phosphorus. Iron was deliberately introduced to these two samples by annealing both wafers at 1273 K (1000 °C) together with Fe-contaminated multicrystalline silicon wafers [16]. The incident flux applied in the

photoluminescence measurement was $1.3 \times 10^{16} \text{ cm}^{-2} \text{ s}^{-1}$ and the total acquisition time was 6 s per data point. Fig. 5 shows the exponential fits of the $\text{Rel}[\text{Fe}_i](t)$ values of both compensated CZ-Si wafers based on an average PL count rate obtained from a $16 \times 16 \text{ mm}^2$ section of the wafers. τ_{assoc} of 161 and 479 s were extracted from these plots, which yield respective N_A values of 1.1×10^{17} and $3.4 \times 10^{16} \text{ cm}^{-3}$. Comparative results of N_A concentrations determined using the photoluminescence technique and previous Quasi-Steady-State Photo Conductance lifetime measurements (QSSPC)[16] are shown in Table 1. The N_A concentrations derived from τ_{assoc} in this experiment were based on the newly revised prefactor B ($5.7 \times 10^5 \text{ s/K cm}^3$) which is 14% higher than the prefactor B ($5 \times 10^5 \text{ s/K cm}^3$), which the N_A

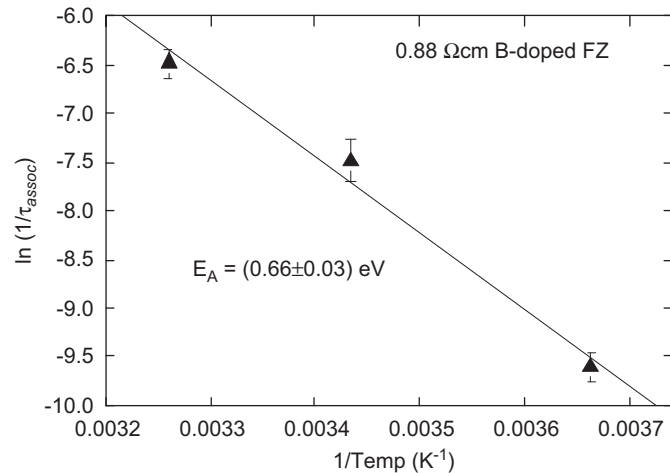


Fig. 4. Arrhenius plot of the pair formation rate for the B-doped FZ sample, giving an activation energy of pair formation of $E_A = 0.66 \pm 0.03 \text{ eV}$.

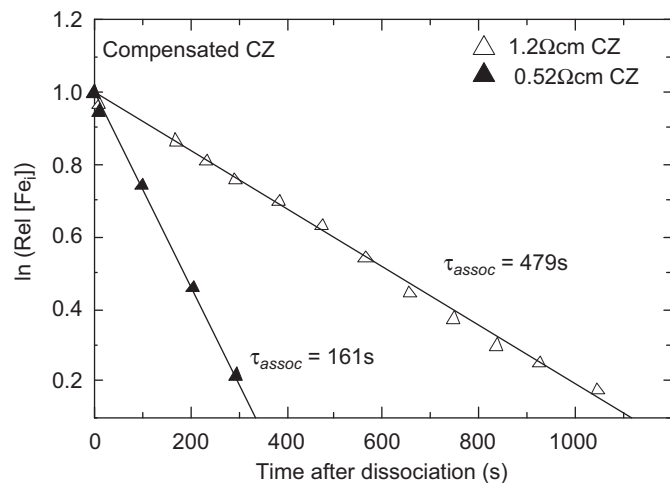


Fig. 5. τ_{assoc} values of 161 and 479 s were obtained for the CZ samples #44 at 302 K (29 °C) and #45 at 303 K (30 °C), which correspond to acceptor concentrations of 1.2×10^{17} and $3.6 \times 10^{16} \text{ cm}^{-3}$, respectively.

concentrations obtained using the QSSPC technique were computed from. Taking this into account, the discrepancy between the two techniques is within 5%, which reflects good agreement between the two techniques. The results confirm that the technique is able to measure the total acceptor concentration N_A , even in the presence of strong compensation.

4.3. Heavily doped upgraded metallurgical graded silicon wafer

The last sample to which the new technique was applied was a passivated CZ grown Upgraded Metallurgical-Grade (UMG-Si) silicon wafer. Fig. 6 shows the time-resolved PL count rate taken from a $25 \times 29 \text{ mm}^2$ section of the sample measured at 274.3 K (1.3 °C) after the complete dissociation of FeB pairs. The incident flux in this measurement was $1.6 \times 10^{17} \text{ cm}^{-2} \text{ s}^{-1}$ and the total acquisition time was 4 s per data point. The FeB re-pairing process was characterised by a time constant of 94 s as obtained from the exponential fit represented by the solid line in Fig. 6. Note that the proportional change in PL counts is much smaller than that for the Fe-implanted FZ sample, since in this case we are relying on the presence of unintended iron in the sample. Nevertheless, the change is sufficiently large to allow reliable extraction of τ_{assoc} .

This τ_{assoc} obtained at 274.3 K (1.3 °C) corresponds to an acceptor concentration of $2.2 \times 10^{18} \text{ cm}^{-3}$. The FeB re-pairing kinetics measurement was repeated at different temperatures. Table 2 lists the τ_{assoc} extracted at the respective temperatures and their corresponding N_A . As expected, the FeB repairing rate increases as a function of temperature. There is some scatter in the data due to the small change in PL intensity. The high repairing rate for temperatures above 287 K (14 °C) makes it difficult for FeB association kinetics to be fully captured experimentally. The average N_A obtained from this experiment, as measured in the temperature range of 274.3 K (1.3 °C) to 287 K (14 °C), was $1.6 \pm 0.7 \times 10^{18} \text{ cm}^{-3}$.

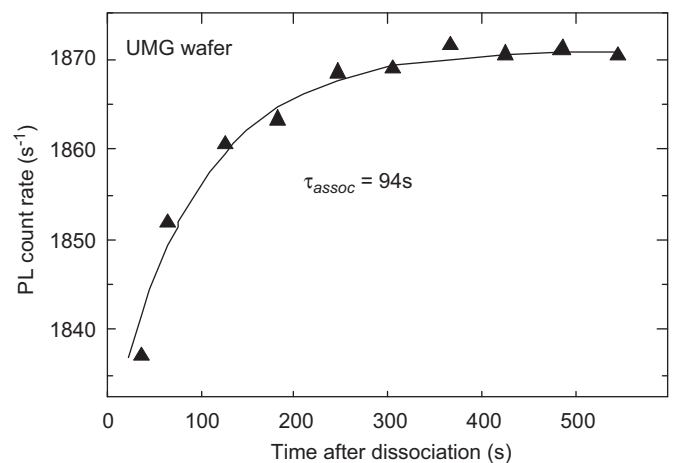


Fig. 6. Time-resolved PL count rate obtained at 274.3 K (1.3 °C) from an upgraded metallurgical-grade silicon wafer, yielding a τ_{assoc} of 94 s.

Table 1

Comparison of N_A concentrations of the compensated CZ samples obtained using quasi-steady-state (QSSPC) and photoluminescence techniques. Resistivities were measured by the four-point-probe method and equilibrium hole concentration p_{OECV} determined by ECV measurements [16].

Wafer	ρ from four-point-probe ($\Omega \text{ cm}$) [16]	p_{OECV} from ECV (cm^{-3}) [16]	$N_D = N_A - p_{\text{OECV}}$ (cm^{-3}) [16]	Compensation ratio $C = N_A + N_D / N_A - N_D$ [16]	N_A (QSSPC technique); (cm^{-3}) [16]	N_A (PL technique); (cm^{-3})
#44	0.52	4.1×10^{16}	5.1×10^{16}	3.5	9.2×10^{16}	1.1×10^{17}
#45	1.2	1.5×10^{16}	1.5×10^{16}	3	3.0×10^{16}	3.4×10^{16}

Table 2

Time constant of FeB formation kinetics for the UMG-Si wafer obtained at different temperatures giving an N_A range of 1.0×10^{18} to $2.4 \times 10^{18} \text{ cm}^{-3}$.

Temperature (K)	τ_{assoc} (s)	N_A (cm^{-3})
274.3 ± 0.3	94	2.2×10^{18}
274.6 ± 0.7	185	1.1×10^{18}
279.9 ± 0.5	130	9.4×10^{17}
280 ± 0.3	58	2.1×10^{18}
286 ± 0.1	47	1.5×10^{18}
287 ± 0.2	44	1.5×10^{18}

Table 3

Inductively coupled plasma mass spectroscopy results for the UMG-Si wafer.

Element	ppb by weight	Concentration (cm^{-3})
^{11}B	10000 ± 2100	$1.3 \pm 0.3 \times 10^{18}$
^{27}Al	370 ± 140	$5.2 \pm 1.9 \times 10^{16}$
^{31}P	3800 ± 680	$1.7 \pm 0.3 \times 10^{17}$

An independent acceptor density measurement was performed on the same sample by using inductively coupled plasma mass spectroscopy (ICP-MS), which gave the elemental analysis results shown in Table 3. The total acceptor concentration measured with this technique was the sum of elements ^{11}B and ^{27}Al , which is $1.4 \pm 0.3 \times 10^{18} \text{ cm}^{-3}$, in good agreement with the average acceptor concentration result measured by using the photoluminescence technique. The results demonstrate that monitoring the iron-acceptor pair formation rate with low injection photoluminescence is a useful, non-destructive tool for determining acceptor concentrations in silicon materials, even when highly doped. Importantly, the technique is applicable irrespective of the presence of compensating dopants, as has been shown previously for the use of QSSPC measurements [2].

5. Conclusion

In this paper, we have introduced a new technique for determining the acceptor concentration in silicon wafers through monitoring the Fe-acceptor kinetics using band-to-band photoluminescence. We have shown that τ_{assoc} derived from this technique, which operates at a constant generate rate, agrees well with τ_{assoc} extracted at a fixed excess carrier density at mid-injection level using QSSPC lifetime measurements. Low injection level measurement conditions are best suited for monitoring FeB kinetics, as unwanted FeB pair re-breaking during the measurement process can be effectively avoided. The photoluminescence technique used here, being immune to minority carrier trapping and depletion region modulation at low injection levels, is thus the ideal tool for this application. The method can be used to determine acceptor concentrations with quite high accuracy, even in strongly compensated wafers or very heavily doped material,

and can sometimes be based on the presence of natural Fe present, rather than requiring the implantation of Fe.

Acknowledgements

The authors would like to thank Dr. Jason Tan, Mr. Christian Samundsett, Mr. S.P. Phang of ANU for their technical support in float zone wafer preparation, Ms. B. Lim of ISFH in compensated Czochralski silicon wafers preparation, and Dr Charlotte Allen of ANU for assisting with ICP-MS measurements. This work has been supported by the Australian Research Council.

References

- [1] A. Istratov, H. Hieslmair, E. Weber, Iron and its complexes in silicon, *Applied Physics A-Materials Science and Processing* 69 (1999) 13–44.
- [2] D. Macdonald, A. Cuevas, L.J. Geerligs, Measuring dopant concentrations in compensated p-type crystalline silicon via iron-acceptor pairing, *Applied Physics Letters* 92 (2008) 202119.
- [3] L.C. Kimerling, J.L. Benton, Electronically controlled reactions of interstitial iron in silicon, *Physica B and C* 116 (1983) 297–300.
- [4] D. Macdonald, T. Roth, P.N.K. Deenapanray, K. Bothe, P. Pohl, J. Schmidt, Formation rates of iron-acceptor pairs in crystalline silicon, *Journal of Applied Physics* 98 (2005) 083509.
- [5] H. Reiss, C.S. Fuller, F.J. Morin, Chemical interactions among defects in germanium and silicon, *Bell System Technical Journal* 35 (1956) 535–636.
- [6] R.A. Bardos, T. Trupke, Self-consistent determination of the generation rate in photoluminescence and photoconductance lifetime measurements, in: *Proceedings of the Conference Record of the Thirty-First IEEE Photovoltaic Specialists Conference*, 2005, pp. 899–902.
- [7] T. Trupke, R.A. Bardos, M.C. Schubert, W. Warta, Photoluminescence imaging of silicon wafers, *Applied Physics Letters* 89 (2006) 044107.
- [8] T. Trupke, R.A. Bardos, Photoluminescence: a surprisingly sensitive lifetime technique, in: *Proceedings of the Conference Record of the Thirty-First IEEE Photovoltaic Specialists Conference*, 2005, pp. 903–906.
- [9] R.A. Bardos, T. Trupke, M.C. Schubert, T. Roth, Trapping artifacts in quasi-steady-state photoluminescence and photoconductance lifetime measurements on silicon wafers, *Applied Physics Letters* 88 (2006) 053504.
- [10] L.J. Geerligs, D. Macdonald, Dynamics of light-induced FeB pair dissociation in crystalline silicon, *Applied Physics Letters* 85 (2004) 5227–5229.
- [11] W. Wijaranakula, The reaction kinetics of iron–boron pair formation and dissociation in p-type silicon, *Journal of The Electrochemical Society* 140 (1993) 275–281.
- [12] J. Tan, D. Macdonald, F. Rougieux, A. Cuevas, Accurate measurement of the formation rate of iron–boron pairs in silicon, *Semiconductor Science and Technology* 26 (2011) 055019.
- [13] G. Zoth, W. Bergholz, A fast, preparation-free method to detect iron in silicon, *Journal of Applied Physics* 67 (1990) 6764–6771.
- [14] D.H. Macdonald, L.J. Geerligs, A. Azzizi, Iron detection in crystalline silicon by carrier lifetime measurements for arbitrary injection and doping, *Journal of Applied Physics* 95 (2004) 1021–1028.
- [15] S. Herlufsen, J. Schmidt, D. Hinken, K. Bothe, R. Brendel, Photoconductance-calibrated photoluminescence lifetime imaging of crystalline silicon, *Physica Status Solidi–Rapid Research Letters* 2 (2008) 245–247.
- [16] B. Lim, A. Liu, D. Macdonald, K. Bothe, J. Schmidt, Impact of dopant compensation on the deactivation of boron–oxygen recombination centers in crystalline silicon, *Applied Physics Letters* 95 (2009) 232109.
- [17] D. Macdonald, J. Tan, T. Trupke, Imaging interstitial iron concentrations in boron-doped crystalline silicon using photoluminescence, *Journal of Applied Physics* 103 (2008) 073710.
- [18] D. Macdonald, T. Roth, P.N.K. Deenapanray, T. Trupke, R.A. Bardos, Doping dependence of the carrier lifetime crossover point upon dissociation of iron–boron pairs in crystalline silicon, *Applied Physics Letters* 89 (2006) 142107.
- [19] E.R. Weber, Transition metals in silicon, *Applied Physics A (Germany)* 30 (1983) 1–22.